Supporting Information

Maseyk et al. 10.1073/pnas.1319132111

Field Site and Instrumentation

Measurements of soil carbonyl sulfide (COS), CO_2, and water fluxes were conducted at the Atmospheric Radiation Measurement Southern Great Plains (SGP) central facility, near Billings, north-central Oklahoma (36.61°N, 97.49°W), where eddy covariance (EC) measurements of ecosystem CO_2 and water fluxes are ongoing (see ref. 1). The field surrounding the EC tower was planted with winter wheat in January 2012. We conducted measurements from April 4 to June 6, 2012 [day of year (doy) 95–159]. There are two gaps in our datasets, due to an intensive field campaign (doy 130–135) and due to the harvest (around doy 145).

High-precision and high-resolution measurements of COS, CO_2, and H_2O were enabled by a Quantum Cascade Laser (QCL) analyzer (CW-QC-TILDAS; Aerodyne Research Inc.). The QCL analyzer produces a high-power, narrow line width beam that passes through a multipass absorption cell (2). An astigmatic Herriott cell provides a path length of 76 m in a 0.5 l volume. Measurements were made at a wavenumber of 2,050 cm^{-1}. Flow through the optical cell was provided by a TriScroll 600 pump (Varian, Inc.) at 6 slm and a pressure of 40 Torr, providing a cell turnover time of 0.166 s.

We used a flow-through soil chamber (LI8100-104C; Li-Cor) coupled to the QCL to measure soil fluxes of COS, CO_2, and water. The chamber was placed on a soil collar located inside the wheat field ∼30 m from the EC tower. The collar was inserted into the ground 6 d before the start of measurements to allow for any disturbance effects to settle. The residence time of air in the tubing between the chamber and QCL was 3–4 s. The air close to the soil was characterized by rapidly fluctuating COS concentrations. To supply the chamber with air containing a stable concentration of COS, the chamber inlet port was connected to tubing drawing air from an inlet at 4 m height on the adjacent EC tower. A three-way solenoid connected the QCL inlet to the chamber outlet line and the EC line.

For an estimate of spatial variability, measurements were made on two additional collars installed within a 20-m radius of the primary collar, also within the wheat field, between days 95 and 100. Fluxes from all three collars were measured within a half-hour period by moving the chamber between collars. Fluxes from the additional collars were correlated with the main primary collar ($r = 0.68$ and 0.82), and the difference between the mean of the three collars and the primary collar was -0.23 ± 2.50 pmol m^{-2} s^{-1} (mean ± SD, $n = 13$) over the set of replicate measurements.

Stomatal conductance was measured on the wheat plants at the site during peak growth at the start of the campaign (doy 92–98) using a LI-6400 portable photosynthesis system (Li-Cor, Inc.). Daytime measurements were made on 10 samples under saturating light and at a stable leaf chamber CO_2 concentration of 380 ppm. Nighttime measurements were made on 12 samples at least 1 h after dark.

Correcting Chamber Effects

The blank effects of the chamber and soil collar were characterized during two intensive measurement campaigns in April and May (Fig. S1) by sealing the bottom of the chamber with an inert base (FEP film; Goodfellow Cambridge Ltd.). Blank chamber tests were done on the automatic program and manually by actuating the chamber for repeated measurements within a short time period. We sometimes observed anomalously low (near zero) fluxes when the chamber was left overnight, which were attributed to condensation (data not shown and not included in regressions). This observation led us to also exclude some nighttime data from the soil flux measurements under similar conditions (with very low or negative water flux values).

We found temperature-dependent COS outgassing by both chamber and soil collar materials. There was good agreement between the two measurement dates and approaches. We derived exponential fits of COS production to the chamber air temperature and used this fit to correct the raw soil flux data. Separate equations were derived for the chamber only and chamber + collar (Fig. S1), and the collar-only effect was estimated by the difference. However, we note that a small bias in the exponential fit could lead to large errors in the flux correction as we extrapolate to very high temperatures (up to 46 °C) during the later parts of the campaign, outside the range of blank chamber measurements. The raw flux data were corrected for the two effects from chamber and collar materials separately. The effects of the chamber were scaled by air temperature. The effects of the collar cannot be scaled simply by soil temperature. This is because during the flux measurements about half of the collar height was inserted into the soil. Thus, the collar effects were scaled 50% each by air and soil temperature. On the other hand, the part of the collar that was inserted into the soil may not contribute fully to the chamber effects if some of its emitted COS is taken up within the soil. Thus, we used the above estimate as the upper limit and only the above-soil section of the collar as the lower limit of COS outgassing from the collar, with the best-estimate correction in between these two limits.

Soil and Ecosystem COS Exchange After Harvest

After harvest, when soil fluxes from the bare field are expected to dominate net ecosystem exchange, there was good agreement of the diurnal pattern and magnitude between the soil fluxes measured with the chamber and net ecosystem fluxes measured by the EC system (Fig. S2). The EC data also confirmed the strong soil source of COS after harvest at the site.

Increased Frequency Measurements

From doy 109–115, we increased the measurement frequency to 15 min (Fig. S3). This confirmed that the main diurnal variability was captured well by our regular 2-h cycle. The average COS flux during the 6 d was 0.53 ± 2.58 pmol m^{-2} s^{-1} for the 15-min data and 0.61 ± 2.45 pmol m^{-2} s^{-1} for the subset of data collected on the regular 2-hourly cycle. Total emissions over this period were 9.6 μg S m^{-2} and 11.2 μg S m^{-2} when calculated from the 15-min data and 2-hourly data, respectively. Average CO_2 fluxes at the two frequencies were within 1% of each other. The COS flux–temperature response does not change between the sampling frequencies (inset, Fig. S3), but there is more variability in the higher-frequency COS data, particularly at the higher uptake rates. The higher variability in the COS data is likely due to the lower precision of these measurements but may also indicate that the higher-frequency measurements were disturbing the soil profile more for COS than CO_2.

Relationship of COS, CO_2, and H_2O Fluxes with Soil Temperature

We found correlations between fluxes and soil temperature that varied with SWC (Fig. S4). For the COS flux, there appears to be a threshold for the soil temperature response between a SWC of 15–20%, with a steeper slope at higher SWC (Fig. S4*A*). However, phenological periods provide a clearer separation than a simple SWC response (Fig. 2). The relationships between CO_2 and water fluxes and soil temperature were similar to that of

COS fluxes but much more noisy (Fig. S4 *B* and *C*). The SWC threshold of CO_2 fluxes vs. soil temperature was also similar (Fig. S4*B*), although the effect of SWC on CO_2 fluxes was greater than for COS. Below the SWC threshold CO_2 fluxes increased with temperature during the first part of the campaign, whereas above the threshold CO_2 fluxes are small, with almost no change with temperature. This behavior started around doy 135 with low soil moisture and very high soil temperature (up to 46 °C). Evaporation was only weakly correlated with soil temperature (Fig. S4*C*). As the soil dried toward the end of the campaign, soil evaporation decreased and therefore did not simply reflect soil temperature.

Temperature Correction for Comparison of Soil and Net Ecosystem Fluxes

For a more appropriate ecosystem soil flux estimate we applied a temperature correction to the soil flux data. Some vegetation had to be cleared for chamber installation, and the temperature of the exposed soil in and around the collar was higher than that beneath the growing wheat canopy (Fig. 1*D*). Therefore, we corrected our measured soil fluxes to those of the below-canopy temperature using regressions obtained from the flux vs. soil temperature relationship (Fig. 2). Two flux–temperature relationships were derived, for SWC above and below 18%, and fluxes were estimated from temperature and SWC data measured beneath the undisturbed canopy as part of the regular ongoing site measurements. The correction was not applied to the postharvest data, when the canopy had been cleared. The total error on the corrected fluxes was determined by propagating the errors from the blank chamber corrections, the replicate chamber measurements, and the temperature corrections. Note that accounting for this correction results in a lower average LRU than the 1.6 presented earlier (3).

Soil COS Emissions

The total emissions estimated for the 7-wk measurement period up until harvest from below the canopy were 355 μg S m^{-2}. Emissions from the bare soil in the 2-wk period following harvest were 304 μg S m^{-2}. These estimates include some gap-filled fluxes using the 30-min soil temperature and SWC data and the observed temperature relationships.

We also estimated the soil COS fluxes for our site based on the approach typically used in regional and global budgets (4). The difference between our observations and this estimate amounts to an additional 820 μg S m^{-2} added to the atmosphere over the period of study.

1. Fischer ML, Billesbach DP, Berry JA, Riley WJ, Torn MS (2007) Spatiotemporal variations in growing season exchanges of CO_2, H_2O, and sensible heat in agricultural fields of the southern great plains. *Earth Interact* 11(17):1–21.
2. McManus JB, et al. (2010) Application of quantum cascade lasers to high-precision atmospheric trace gas measurements. *Opt Eng* 49(11):111124.
3. Billesbach DP, et al. (2014) Growing season eddy covariance measurements of carbonyl sulfide and CO_2 fluxes: COS and CO_2 relationships in Southern Great Plains winter wheat. *Agric For Meteorol* 184:48–55.
4. Kettle AJ, Kuhn U, von Hobe M, Kesselmeier J, Andreae MO (2002) Global budget of atmospheric carbonyl sulfide: Temporal and spatial variations of the dominant sources and sinks. *J Geophys Res* 107(D22):4658.

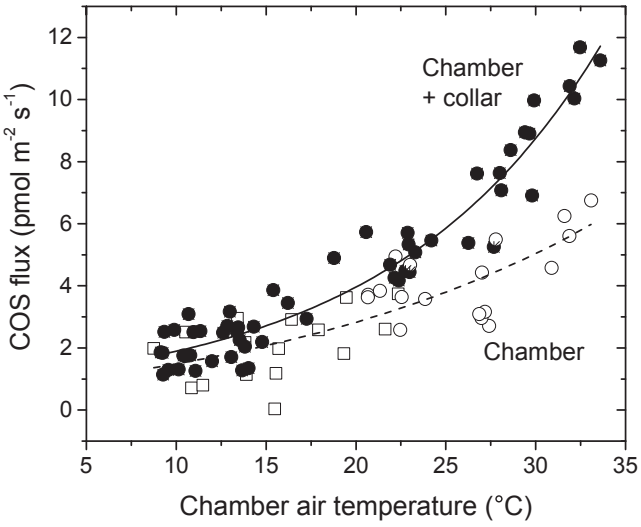

Fig. S1. COS produced by the chamber and soil collar depending on chamber air temperature. Tests were conducted in April (squares) and May (circles). Exponential regression curves were obtained from the chamber and chamber + collar data and used to correct measured soil fluxes: chamber flux = −1.75 + $2.51e^{0.031T}$ (r^2 = 0.62) and chamber + collar flux = 1.54 + $0.28e^{0.106T}$ (r^2 = 0.93), where T is temperature (°C).

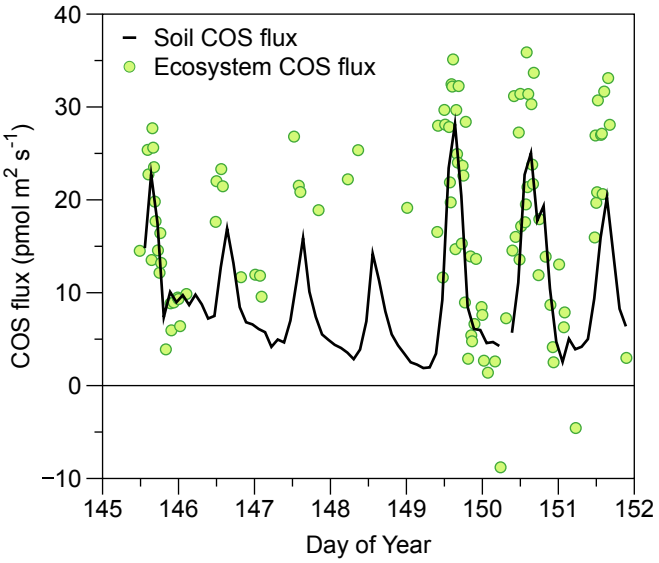

Fig. S2. Soil COS fluxes measured with the soil chamber agree well with net ecosystem fluxes measured by the EC system after harvest, when the soil dominates ecosystem fluxes. Note that this figure shows a detail from Fig. 1.

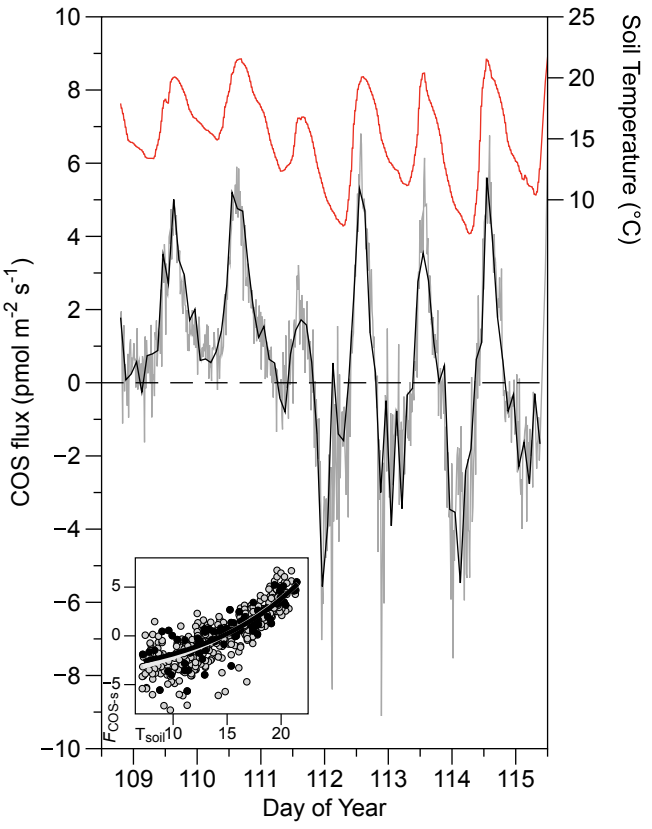

Fig. S3. Comparison of high-frequency soil measurements (15 min; gray line) to those on the regular 2-h cycle (black line) demonstrates that the regular 2-h schedule was able to capture the main diurnal variability of soil COS fluxes, which is strongly related to temperature (red line). The fitted equations of the flux–temperature response (inset) are $-6.82 + 2.00e^{0.0847Tsoil}$ ($r^2 = 0.71$, sd = 1.38) for the 15-min data (gray) and $-4.74 + 0.97e^{0.1097Tsoil}$ ($r^2 = 0.70$, sd = 1.33) for the 2-h data (Fig. 3). Note that this figure shows a detail from Fig. 1.

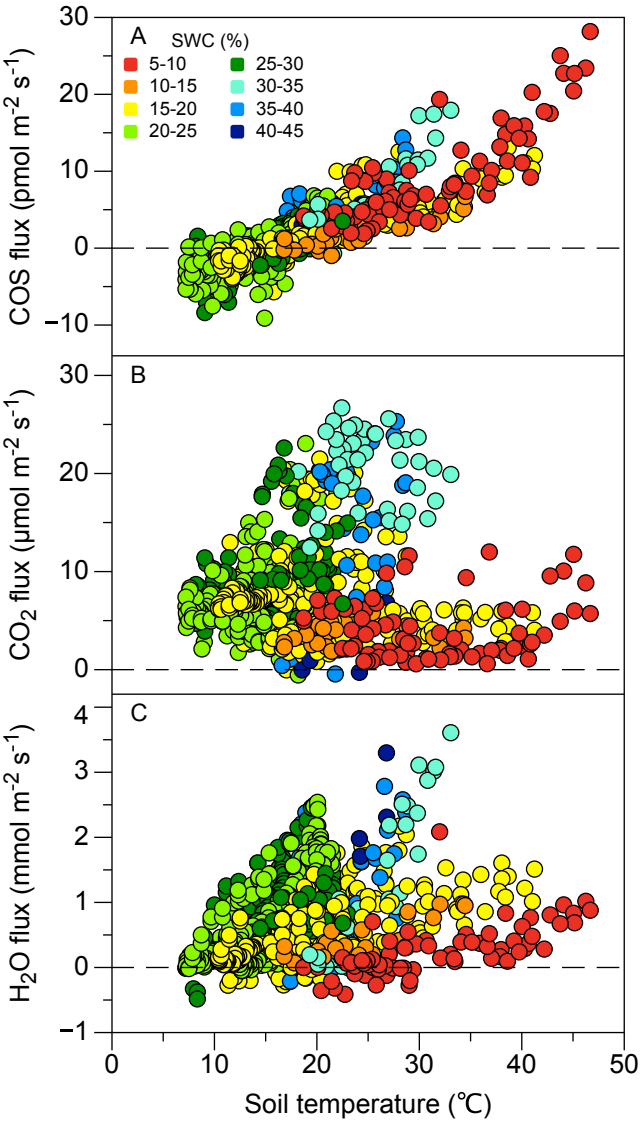

Fig. S4. Relationship between soil temperature and soil fluxes of COS (*A*), CO_2 (*B*), and water (*C*) depending on soil water content (SWC). The flux vs. temperature relationships have a threshold at SWC of 15–20%, with larger slopes above the threshold.